

TOWARD AUTONOMOUS PHOTOVOLTAIC BUILDING ENERGY MANAGEMENT: MODELING AND CONTROL OF ELECTROCHEMICAL BATTERIES

Hoang-Anh Dang, Benoit Delinchant, and Frederic Wurtz
G2Elab, Grenoble University, Grenoble, France

ABSTRACT

In building energy management, the electrochemical battery is important to ensure power supply continuity and reduce cost of electrical consumption. Therefore, an electrical model of battery is highly recommended for our main objectives, which can contribute to simulate the impact of electrical storage in the building.

In this paper, we present the modelling and application of electrochemical battery used in a building (the building PREDIS of Grenoble University). In our experimental platform, we have several laptops connected, with their electrical storage capabilities, to the electrical system. In which, we simulate a typical day of photovoltaic generation.

INTRODUCTION

A smart building is a type of building that, from design, technologies and building products, uses less energy than a conventional building and can be controlled optimally by occupant. Energy management is one of innovate solutions to reach this goal within two main strategies:

- Reduce energy consumption and develop renewable sources
- Optimize power supply that depends on production, distribution and storage.

To assess the potential gains from these solutions, one of priorities is the development of simulation models, which could be used for global simulation, optimization and prediction for energy management in buildings.

Nowadays, the portable devices (laptop, smart phone, tablet, electrical vehicle...) are very popular and multiply the energy consumption in building. Their battery could be used to control their energy profile consumption and autonomous renewable resources (e.g. Celik, 2002). Electrical storage modelling becomes to be important in our development of simulation models.

MODELLING

In simulation and application of electrical storage, the preferred electrical model of battery is electrical capacity, which is simple and describes energy balance in charging and discharging process. However, this model cannot describe accurately the functional states of the battery at each moment (state of charge, state of health) and some functional conditions

(overtoltage, overcurrent) for predictive and feedback control. For example (Figure 1), in the constant voltage stage, charge current depends highly on battery property, and real charge time is much longer than estimated charge time by using an electrical capacity model. To reach these proposed goals and take into account the battery typical characteristics, a physical model is required but has to be as simple as possible.

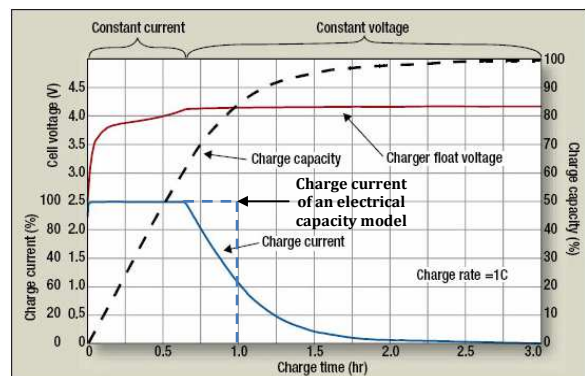


Figure 1 Charge profile of a Li-ion battery
(Source: powerelectronics.com)

Functional specification

Specifications of this model is designed to fit a large scale of operations in different scenarios. The input data is the power set point (P_{sp} : positive in discharge mode and negative in charge mode) and output data are real battery power (P_b), state of charge (SOC), state of health (SOH), Joule losses, available discharge power and available charge power. (Figure 2)

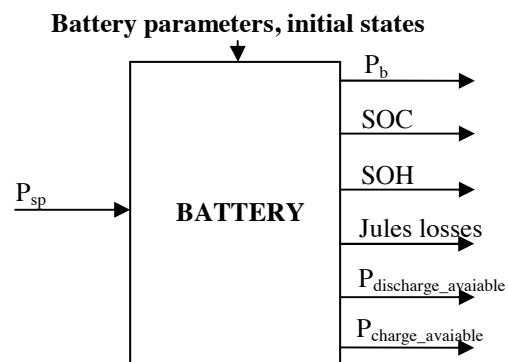


Figure 2 Battery model specification

As a physical battery, the following constraints must be satisfied:

- Charge power should not cause overvoltage ($V \leq V_{\max}$),
- The charging current does not exceed a limit value ($I \leq I_{\lim}$).

In case of a discharge or charge power greater than the available value, the model will only provide its available power. Moreover, to preserve battery life-time, model will decide to disconnect battery from electrical load when the state of charge is too low ($SOC = SOC_{\min}$).

Electrical equivalent model

Various models are available in the literature (e.g. Guasch et al., 2011) to reach fine and fast simulation. In our framework, a simple model is preferred to describe charging and discharging process. This is the reason why we have chosen Shepherd's hypothesis (e.g. Shepherd, 1963) as the basis content of this model. These hypothesis are based on a simple equivalent circuit: a voltage source is connected with a variable resistor. (Figure 3)

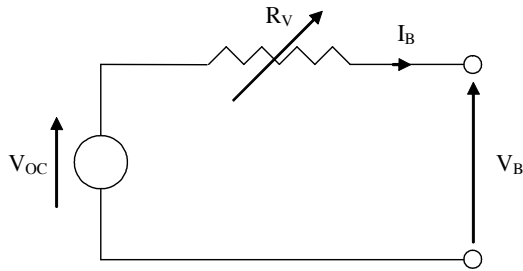


Figure 3 Electrical equivalent circuit

This model must take into account the variation of battery voltage depending on battery state of charge. Indeed, the curve consists of three operating zones: exponential zone, nominal zone and polarization zone. (Figure 4)

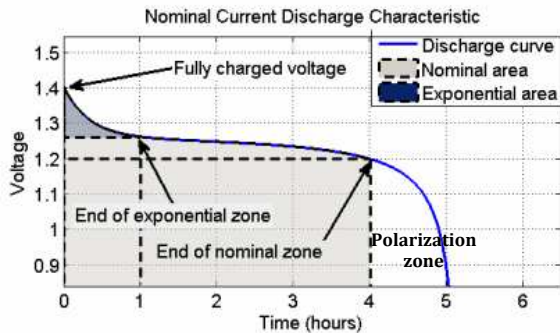


Figure 4 Typical Discharge Curve Characteristics

By synthesizing the three discharge phenomena and Shepherd's hypothesis, we can re-establish power discharging and charging equations (e.g. Tremblay et al., 2007).

For the discharge mode ($I_B \geq 0$), the battery power equation across the battery can be defined as below:

$$P_B = V_0 I_B - R_I I_B^2 - K \frac{Q_{\max}}{Q} I_B^2 + A I_B e^{B(Q-Q_{\max})} \quad (1)$$

In charge mode ($I_B \leq 0$), the polarisation resistor is modified to approach the operation of the battery. So the power equation is rewritten:

$$P_B = V_0 I_B - R_I I_B^2 - K \frac{Q_{\max}}{Q_{\max} - Q} I_B^2 + A I_B e^{B(Q-Q_{\max})} \quad (2)$$

These equations allow determining the state of charge (SOC), the available powers (charge and discharge) and Joule losses.

State of charge:

$$SOC = \frac{Q}{Q_{nom}} \times 100\% \quad (3)$$

Joule losses in discharge mode:

$$Joule\ losses = R_I I_B^2 + K \frac{Q_{\max}}{Q} I_B^2 \quad (4)$$

Joule losses in charge mode:

$$Joule\ losses = R_I I_B^2 + K \frac{Q_{\max}}{Q_{\max} - Q} I_B^2 \quad (5)$$

Available discharge power:

$$P_{\text{discharge_available}} = \frac{[V_0 + A I_B e^{B(Q-Q_{\max})}]^2}{4(R_I + K \frac{Q_{\max}}{Q})} \quad (6)$$

Available charge power at constant current stage:

$$P_{\text{charge_available}} = V_0 I_{B_lim} - R_I I_{B_lim}^2 - K \frac{Q_{\max}}{Q_{\max} - Q} I_{B_lim}^2 + A I_{B_lim} e^{B(Q-Q_{\max})} \quad (7)$$

Available charge power at constant voltage stage:

$$P_{\text{charge_available}} = - \frac{V_{\max}^2 - V_{\max} V_0 - V_{\max} A e^{B(Q-Q_{\max})}}{R_I + K \frac{Q_{\max}}{Q_{\max} - Q}} \quad (8)$$

Besides, the state of health (SOH) is estimated by "additive law" (e.g. Picciano, 2007):

$$SOH = \left[1 - \frac{\int I_B dt}{N_C \times Q_{\max}} \right] \times 100\% \quad (9)$$

The model can accurately simulate the behaviour of an electric battery by using identified parameters from typical battery characteristics.

In our framework, we have to keep a compromise between accuracy and ease of use. In particular, model parameters can be considered constant in charge mode and discharge mode, thus facilitating the implementation of the model. Our model inte-

grates the parameters for four famous kind of battery (Lead-acid, Ni-Cd, Ni-Mh, Li-ion)

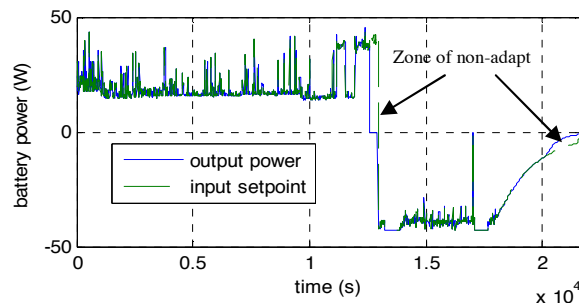
Table 1 gives typical values of parameters for each technology of battery and those values are especially defined by solving the system of equation (1) applied for different estimated discharge characteristic points (e.g. Tremblay et al., 2009).

Table 1
Electrical costs comparison

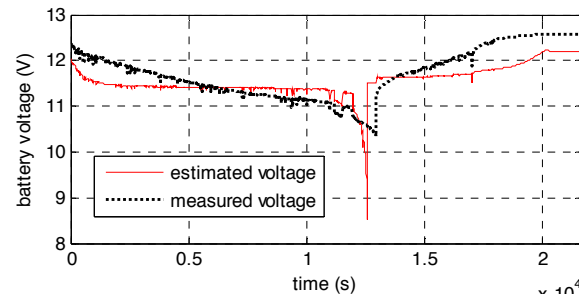
Type	Lead-acid	Ni-Cd	Ni-Mh	Li-ion
Parameters	12V 7.2Ah	1.2V 2.3Ah	3.3V 2.3Ah	1.2V 6.5Ah
V_0 (V)	12.4659	1.2705	3.366	1.2816
R_I (Ω)	0.04	0.003	0.01	0.002
K (Ω or $V/(Ah)$)	0.047	0.0037	0.0076	0.0014
A (V)	0.83	0.127	0.26422	0.111
B (Ah) ⁻¹	125	4.98	26.5487	2.3077

MEASUREMENT CONFRONTATION

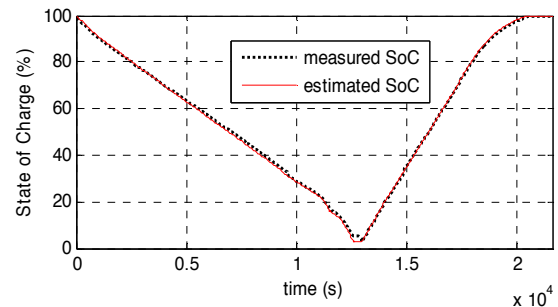
This model is validated by a test on a Laptop DELL Latitude E6400 including a Li-ion battery (rated voltage: 11.1 V, rated capacity: 6100 mAh, cycle durability 1200, initial state of charges 100%). Measurements are obtained by BatteryMon software (v2.1, www.passmark.com).



(a)



(b)



(c)

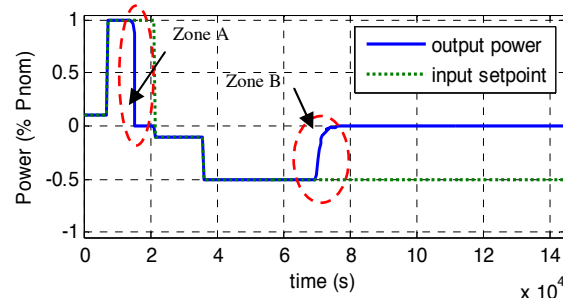
Figure 5 Confrontation simulations/measures

In Figure 5, the simulation is well reproducing the measured power set point and the measured state of charge. Because of using average parameters for Li-ion battery, the model cannot reproduce exactly the battery voltage which is very sensible with different parameter values. This has an influence for calculating the state of charge which is sometimes a little bit higher or lower than measurement data. This is also the case for the output power which cannot reproduce exact values at the end of discharge mode or charge mode as shown on Figure 5.a.

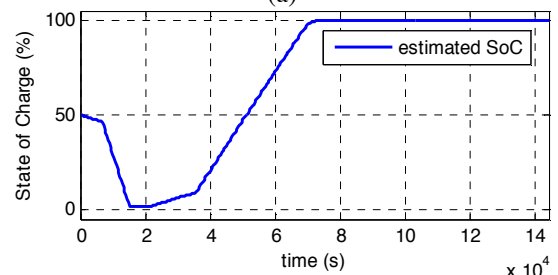
For health protection, the battery should not be used until the end of its charge like it was done in this test case. Thus the peak estimated voltage at end of battery charge (see Figure 5.b) would not exist in almost operation modes. Thus, if we exclude this peak value, Figure 5.b shows that the difference between simulations and measurements is lower than 10% which is the level of accuracy that we can accept.

SIMULATION IN DIFFERENT MODES

To survey available power in operation, the simulation test on Figure 6 illustrates set point powers for low and high demand for a battery with the following parameters: Ni-Cd, 4200mAh and initial SOC = 50%.



(a)



(b)

Figure 6 Power and state of charge in different modes

Figure 6.a, shows that the battery can provides a power that is lower than set point value (see zone A and zone B). Therefore, this demonstrates that our model allows calculating real battery power at the end of discharging or charging processes, this is important to decide the optimal control in building energy management.

IMPLEMENTATION IN PREDIS

The PREDIS “smart building” (PREDIS SB) is situated in Grenoble Electrical Engineering Laboratory (G2Elab). It is a building used for our researches on (building + grid) smart system. Battery modelling and control is one of research activities of this project.

To realize application of battery control strategy, a part of this platform is used as a computer room with laptops and controllable switches.

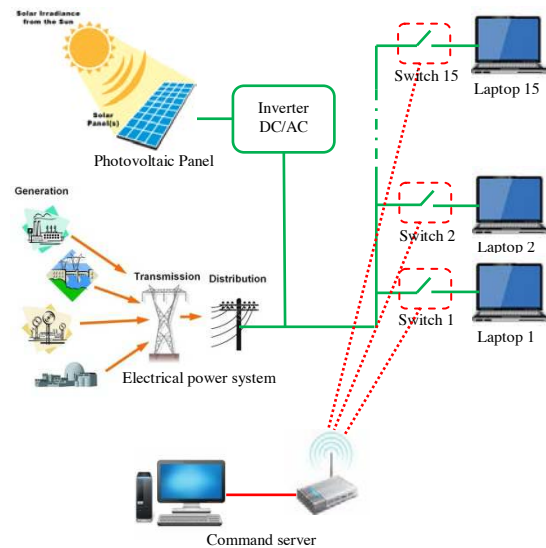


Figure 7 Electrical distribution and control protocol
PREDIS Smart Building

Figure 7 describes an electrical distribution system. We simulate a photovoltaic generation supply for the 15 laptops with a curve of generated power for 1 day illustrated on Figure 9. A command server sends wireless ON/OFF signal to each switch to decide charging/discharging mode of each laptop. These commands are decided in order that the generated power should be consumed as much as possible in the laptops in order to minimize the consumption from the grid. The goal is to reach, or to be closer as possible from the photovoltaic autonomy (Kazema et al. 2013). Therefore, our objective is to define an autonomous and optimal control strategy by using battery model from a proposed scenario and initial battery states.

Technical details:

- Laptop DELL Precision, battery module KY265, type Li-ion, 11.1 V, 85Wh
- Photovoltaic panel : $P_{max} = 1000W$

Our first application is realized by a simulation on a typical day in 2012 November. The total load (Figure 8) is summed from wattmeter measurements of each laptop (Figure 15) at 100% state of charge in order to retrieve pure user load consumption (without battery charge consumption). Besides, the photovoltaic power is estimated from statistical data in 2011 (Figure 9) and the electrical price is given by www.epexspot.com (Figure 10). Initial states of charge for each battery are initialised differently (Figure 14).

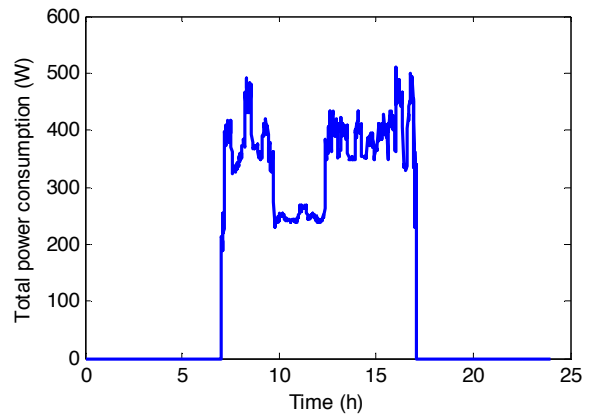


Figure 8 Total load consumption by laptop device

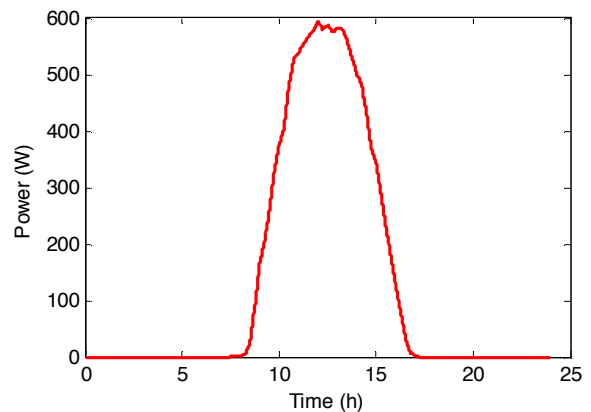


Figure 9 Photovoltaic power

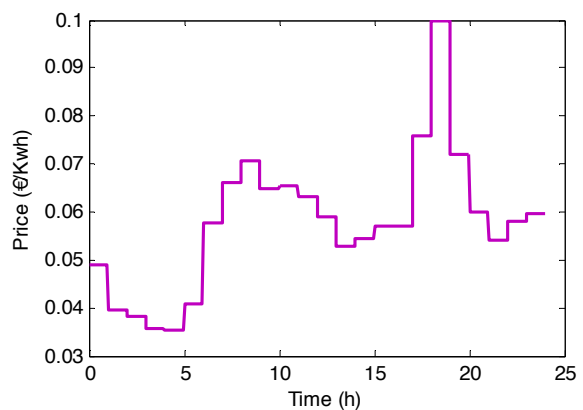


Figure 10 Electrical price

To reach the goal of this application, the control strategy must be deduced by following two steps:

predictive and feedback control. The predictive control calculates energy balance from data prevision and allows preparing necessary energy in battery for whole day operations. In this case, the battery model is used to define charge time and to decide when each laptop should be charged from electrical price evolution. Further, the feedback control decides what laptop can be charged or discharged in each checkpoint time (frequency : each 6 minutes). For this goal, this model is also used to calculate or predict battery states at next time.

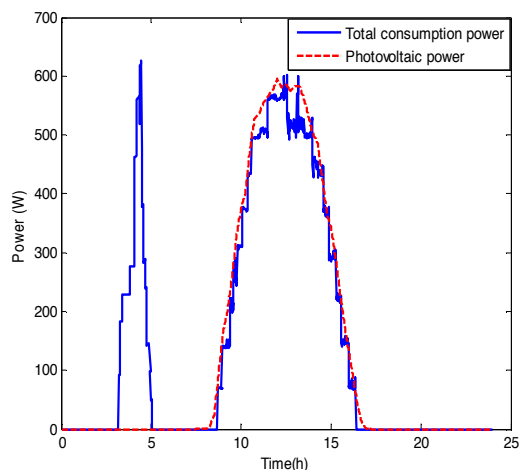


Figure 11 Total power consumption at electrical outlet and photovoltaic power

Figure 11 shows total power consumption before switch device. By using batteries and an optimal control, the power consumption profile can benefit as much as possible from the generated power of the photovoltaic panel maximising by this way the photovoltaic autonomy. Because the energy consumption in this case is more than the generated energy, this system need still buy energy from electrical grid to store on laptop battery, so here the photovoltaic autonomy is not complete.

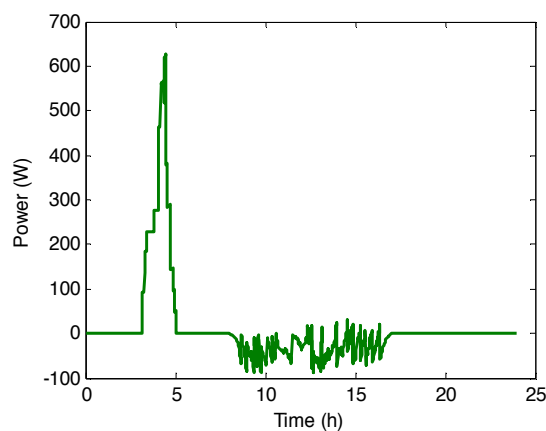


Figure 12 Electrical grid power

From Figure 12, the necessary power is bought at the cheapest moment (3:00am to 5:00am) to minimize

costs. Sometime, we can sell generated power to grid but in reality, this power is used locally for other consumptions (HVAC, lighting...). To understand the gains of this application, the table below compares our strategy to the classical case (PC without electrical storage). The cost gain is about 10 times.

Table 2

Electrical costs comparison

	COST PER MONTH (€)	RATIO
CLASSICAL CASE	6.4	10.67
PREDIS CASE	0.6	1

CONCLUSION

The battery model developed is simple enough to be implemented only from the typical characteristics of the battery and its nominal variables. However, it remains sufficiently realistic regarding the evaluation of battery power, which depends on the state of charge. This model has been validated and used to test different strategies for energy management in PREDIS platform in order to maximise the photovoltaic autonomy. It could also be implemented in optimal management strategies integrating optimization algorithms and storage systems sizing tools. Thus, the proposed model, and the proposed management strategy are a contribution to the problematic of energy autonomy that will an import research topic for the next years.

NOMENCLATURE

$V_{OC} = V_0 + A e^{B(Q-Q_{max})}$ = open circuit voltage (V)

$R_V = R_I + K \frac{Q_{max}}{Q}$ = variable resistor (Ω)

V_0 = constant voltage (V)

R_I = internal resistor (Ω)

K = polarisation voltage factor (V)

I_B = battery intensity (A)

Q_{max} = maximum capacity (Ah)

Q_0 = initial charge (Ah)

$Q = Q_0 - \eta_C \int_0^t I_B dt$ = instantaneous charge (Ah)

(e.g. Valøen et al., 2007)

η_C = Faradaic efficiency

A = voltage factor (V)

B = charge factor (Ah^{-1})

N_C = Cycle durability

REFERENCES

Celik, A.N. Dec 2002. Optimisation and techno-economic analysis of autonomous photovoltaic-wind hybrid energy systems in comparison to single photovoltaic and wind systems, Sci-

enceDirect, volume 43, issue 18, pages 2453-2468.

Shepherd, C.M. May 2 1963. Theoretical design of primary and secondary cells, part III - battery discharge equation, internal report, U. S. naval research laboratory.

Tremblay, O., Dessaint, L.A., Dekkiche, A.I. Sept 9-12 2007. A Generic Battery Model for the Dynamic Simulation of Hybrid Electric Vehicles, IEEE VPPC 2007, pages 284 – 289.

Tremblay, O., Dessaint, L.A May 13-16 2009. Experimental Validation of a Battery Dynamic Model for EV, World Electric Vehicle Journal, volume 3, SSN 2032-6653.

Guasch, D., Silvestre, S. May 2003. Dynamic Battery Model for Photovoltaic Applications, Progress in Photovoltaics: Research and Applications, Volume 11, Issue 3, pages 193–206.

Valøen, L.O., Shoesmith, M.I., Nov 2007. The effect of PHEV and HEV duty cycles on battery and battery park performance, PHEV 2007 Conference, Winnipeg, Manitoba Canada.

Long L. Aug 23 2011. A Practical Circuit based Model for State of Health Estimation of Li-ion Battery Cells in Electric Vehicles, Master of Science thesis, TU Delft, Netherlands.

Picciano N. 2007. Battery Aging and Characterization of Nickel Metal Hydride and Lead Acid, The Ohio State University, USA.

Kazema H. A., Khatiba T., Sopianb K.. June 2013. Sizing of a standalone photovoltaic/battery system at minimum cost for remote housing electrification in Sohar, Oman, Energy and Buildings, Vol. 61, pp 108–115.

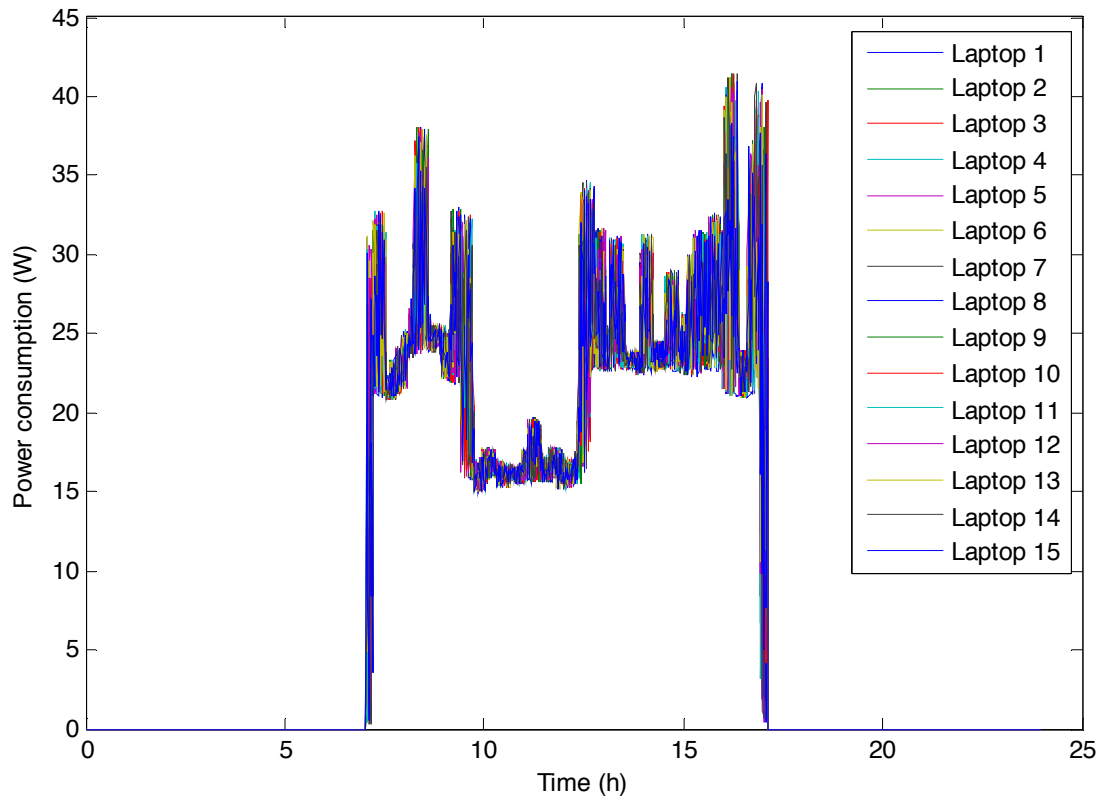


Figure 13 Load consumption of each laptop device

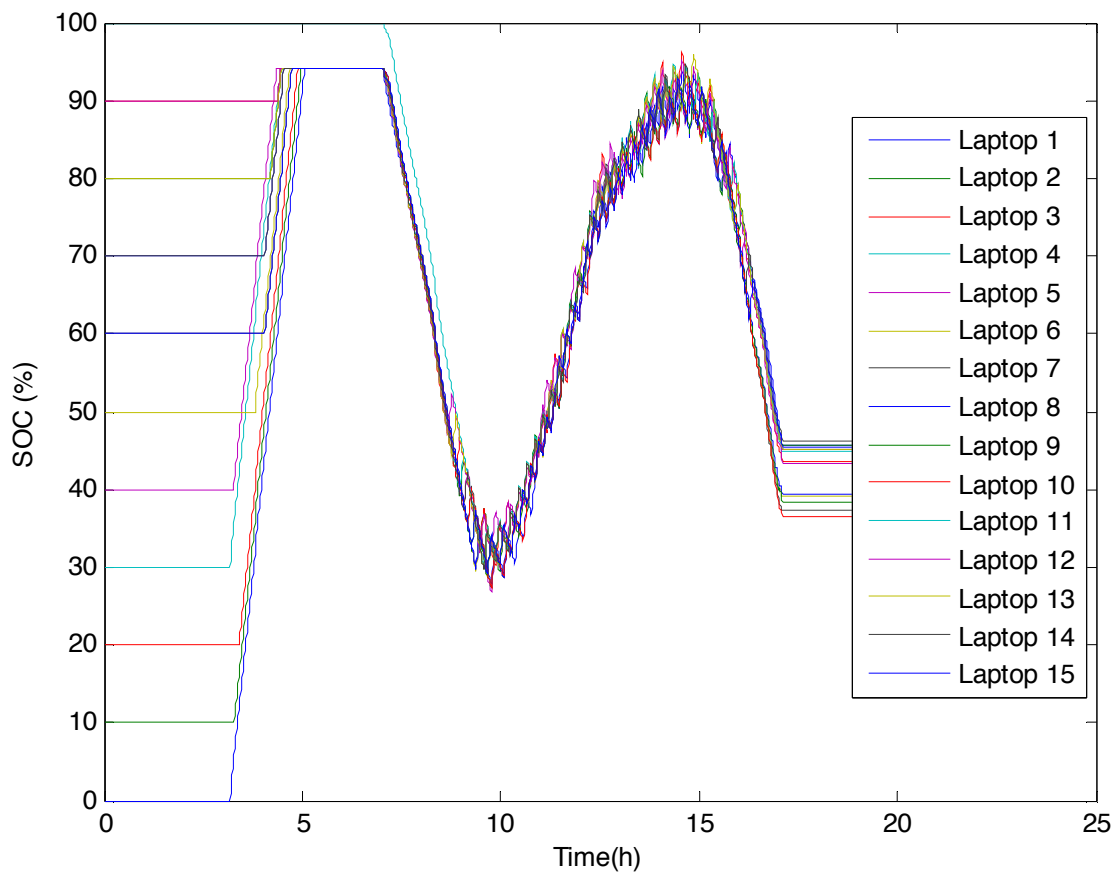
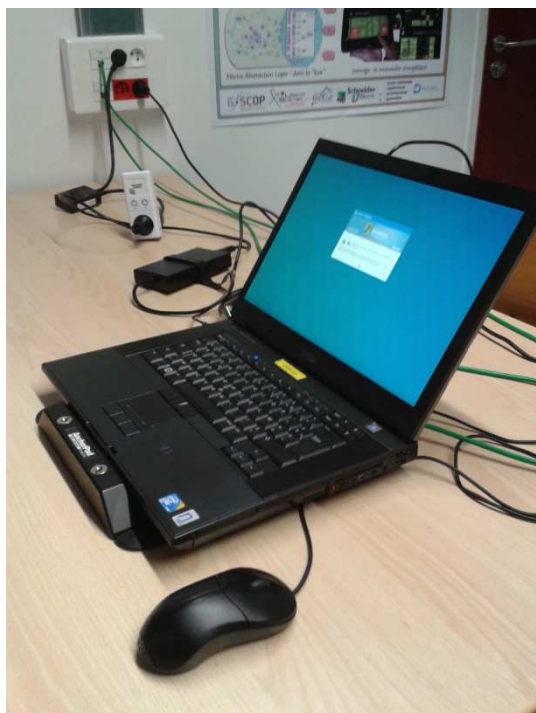


Figure 14 State of charge of each laptop device



(a)



(b)

Figure 15 Laptop, wattmeter and contactor



Figure 16 Computer room